INSTITUTE OF PHYSICS PUBLISHING JOURNAL OF PHYSICS: CONDENSED MATTER

J. Phys.: Condens. Matter **18** (2006) 2601–2614 doi:10.1088/0953-8984/18/8/021

Computing conductances of tunnel junctions by the Korringa–Kohn–Rostoker method: formulation and test of a Green function approach

J Henk, A Ernst, K K Saha and P Bruno

Max-Planck-Institut für Mikrostrukturphysik, Weinberg 2, D-06120 Halle (Saale), Germany

E-mail: henk@mpi-halle.de

Received 9 December 2005
Published 10 February 2006
Online at stacks.iop.org/JPhysCM/18/2601

Abstract

An approach to computing conductances of tunnel junctions within the framework of the Landauer–Büttiker theory for electronic transport is introduced and formulated for the Korringa–Kohn–Rostoker (KKR) method for electronic-structure calculations. After a general introduction to the idea behind the approach, tests and comparisons with other methods, namely a 'transmission of Bloch-waves' approach and an approach based on the Kubo–Greenwood formula for the conductivity tensor, reveal a high accuracy and robustness of the proposed method, thus proving its suitability for state-of-the-art computations of spin-dependent ballistic transport. Based on Green functions, it is flexible and can easily be implemented in present KKR computer codes.

1. Introduction

The enormous progress in the development of magneto-electronic applications is accompanied by a considerable number of theoretical investigations [1]. Besides model calculations which focus on fundamental effects of spin-dependent ballistic transport, transport coefficients of specific systems are computed from first principles, in particular for tunnel junctions. Such a calculation is typically subdivided into two steps. First, the electronic and magnetic properties of the system under consideration are computed self-consistently within density-functional theory, thus providing a state-of-the-art description of the electronic states. The conductance is subsequently computed in the second step, using the *ab initio* results as input. Often, the Landauer–Büttiker theory is used in the second step, in which 'conductance is viewed as transmission' through the tunnel barrier [2].

In the conductance calculations one needs to take into account the boundary conditions that are dictated by the Landauer–Büttiker description of transport. Therefore, one needs an accurate, flexible (boundary conditions) and fast (large system size) computational method. Regarding tunnelling as a scattering process, one obvious choice is multiple-scattering theory,

namely the Korringa–Kohn–Rostoker (KKR) method [3] or one of its derivatives (e.g. screened KKR or layer KKR) [4–6]. These methods were successfully applied to a variety of problems (without any claim of completeness we refer to references [7–14]).

There are two main approaches for computing the conductance of a device with the KKR method. In the first one, one starts from the Kubo–Greenwood formula for the conductivity tensor, which involves matrix elements of the current operator [7]. This expression is then reformulated in order to compute the current flowing through the device, giving eventually the conductance C (see, e.g., [15, 16]). This approach relies on KKR Green functions and was also proposed by and implemented in screened KKR by Mavropoulos *et al* [17].

In the other main approach, one counts the electrons which are transmitted through the device upon connecting it to the leads. Therefore, one needs to compute the transmission probability which determines the conductance, as in the work of Landauer and Büttiker [2, 18]. Following this idea, MacLaren *et al* [19] proposed and implemented a calculational scheme which uses typical layer-KKR algorithms for computing the Bloch states in the leads and the scattering matrix of the tunnel barrier [20]. The latter is expressed in the basis of the Bloch states and, hence, gives the transmission probabilities of the scattering channels. An important feature of this approach is that it directly computes the Bloch states rather than the Green function of the system.

Note further that there are two principal ways to treat disorder in the system. First, in a supercell approach one has to compute the properties of various configurations. The conductance is eventually obtained by averaging over these configurations. Second, using Green functions, one can apply standard techniques for disorder, typically the coherent potential approximation [5, 6, 21, 22] (for a KKR-based approach, see reference [23, 24]). Since the CPA is a widely used technique within the KKR framework, it is desirable to have a method at hand which is based on Green functions.

All the KKR approaches for conductance calculations mentioned so far have specific advantages and disadvantages. In this paper, a Landauer–Büttiker approach which is usually used in the framework of tight-binding [25] is proposed and formulated within the KKR framework. As will be shown, it is as accurate as the MacLaren approach [19] but uses Green functions, thus allowing for a treatment of disorder within the coherent potential approximation. The approach is flexible; for example, it can be used for planar tunnel junctions, scanning tunnelling microscopes or nanowires. Further, it can be implemented in both conventional (three-dimensional) KKR and (two-dimensional) layer-KKR computer codes.

An essential feature of the approach proposed in this paper is that it uses two systems, one with the leads decoupled from the tunnel barrier, the other with the leads coupled to the barrier. This idea was already used by Pendry and co-workers [26] to formulate a theory of the scanning tunnelling microscope. In that publication, a single 'impermeable membrane' was erected between the two leads in order to establish the decoupling. Further, a formulation in multiple-scattering theory was introduced, addressing in particular the effect of a residual (i.e. non-perfect) decoupling. As we will show for our approach, the residual error can be made as small as wanted. A similar method was introduced by Wang and co-workers ([27]; see also the appendix of [28]) for the study of the effect of electronic states localized at the lead surfaces on the conductance. Mainly, because a restriction to nearest-neighbour interactions leads to unacceptable numerical errors, the authors did not recommend that method. The approach presented here, however, does not rely on any assumption typical for tight-binding-like methods.

The paper is organized as follows. In section 2, the approach is outlined, first in general form (section 2.1), second within KKR (section 2.2). Notes and hints on implementation close this section (section 2.3). To prove that the approach is suitable for conductance calculations,

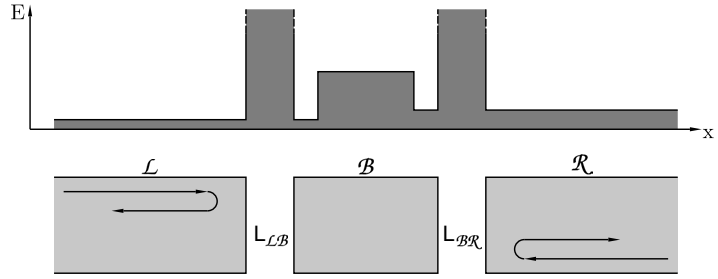

Figure 1. The decoupled system. Bottom: electrons incoming either from the left lead $\mathcal{L}$ or from the right lead $\mathcal{R}$ are completely reflected at the respective lead surfaces. Hence, there is no transmission through the tunnel barrier $\mathcal{B}$ from one lead to the other. The decoupling regions are denoted $\mathsf{L}_{\mathcal{LB}}$ and $\mathsf{L}_{\mathcal{BR}}$. Top: sketch of the potential. The decoupling of the subsystems is established by potential walls of infinite height located at $\mathsf{L}_{\mathcal{LB}}$ and $\mathsf{L}_{\mathcal{BR}}$.

its accuracy is tested (section 3.1) by comparing its results with those of other approaches. Since screened KKR has become a standard calculational scheme for treating large systems, the effect of the screening transformation on the conductance is discussed, too (section 3.2). Concluding remarks are given in section 4.

2. Theoretical

The presented approach relies on the 'electron counting' view of the Landauer–Büttiker theory. Therefore, one has to use two systems: one with the tunnel barrier decoupled from the leads, the other with the tunnel barrier coupled to the leads.

In the general outline (section 2.1), a schematic tight-binding-like formulation of the theory is used, for reasons of simplicity and brevity. We would like to emphasize that the purpose of that section is mainly to introduce the concept of decoupling–coupling. The KKR formulation (section 2.2) uses by no means any approximation typical for tight-binding (e.g. restriction to nearest-neighbour shells or energy-independent basis set). We further note in passing that the idea of connecting the decoupled barrier subsystem to the leads, and thereby changing the boundary conditions, is similar to the 'embedding potential' method [29–31].

2.1. General formulation

2.1.1. The decoupled system. The decoupled system comprises the left lead $\mathcal{L}$, the right lead $\mathcal{R}$ and the tunnel barrier $\mathcal{B}$ (figure 1, bottom). The latter subsystem can comprise either a tunnel barrier (as in a planar junction or in a scanning tunnelling microscope) or a nanowire. Because the three subsystems are isolated from each other (regions $\mathsf{L}_{\mathcal{LB}}$ and $\mathsf{L}_{\mathcal{BR}}$), there is no transport from $\mathcal{L}$ to $\mathcal{R}$ via $\mathcal{B}$ and vice versa. The total Hamiltonian $H_{\rm dc}$ can be expressed schematically in matrix form as

$$H_{\rm dc} = \begin{pmatrix} h_{\mathcal{L}} & 0 & 0 \\ 0 & h_{\mathcal{B}} & 0 \\ 0 & 0 & h_{\mathcal{R}} \end{pmatrix}, \tag{1}$$

where $h_{\mathcal{S}}$ describes the isolated subsystem $\mathcal{S} = \mathcal{L}, \mathcal{B}, \mathcal{R}$. The associated resolvent $G_{\rm dc}(z) = (z - H_{\rm dc})^{-1}$ takes the same form as $H_{\rm dc}$, namely

$$G_{\rm dc}(z) = \begin{pmatrix} g_{\mathcal{L}}(z) & 0 & 0 \\ 0 & g_{\mathcal{B}}(z) & 0 \\ 0 & 0 & g_{\mathcal{R}}(z) \end{pmatrix}, \tag{2}$$

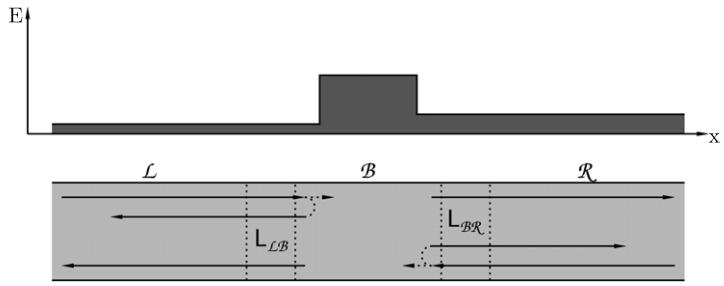

Figure 2. The coupled system. Bottom: because the regions $\mathsf{L}_{\mathcal{LB}}$ and $\mathsf{L}_{\mathcal{BR}}$ allow now for transport (see figure 1), electrons incoming from either of the leads can pass through the tunnel barrier $\mathcal{B}$ but are partly reflected. Hence, there is transmission from one lead to the other through $\mathcal{B}$. Top: the coupling of the subsystems is established by replacing the potentials walls in $\mathsf{L}_{\mathcal{LB}}$ and $\mathsf{L}_{\mathcal{BR}}$ (figure 1, top) by the lead potentials.

with $g_{\mathcal{S}}(z) = (z - h_{\mathcal{S}})^{-1}$ and z a complex number. In this schematic tight-binding formulation, $h_{\mathcal{S}}$ (and correspondingly $g_{\mathcal{S}}$) can be regarded as a matrix which describes the hopping in the bulk and at the surface of lead $\mathcal{S} = \mathcal{L}, \mathcal{R}$. Its explicit form need not be specified because this is not necessary for the derivation of the conductance expression, equation (8).

The decoupling can be accomplished by potential barriers of infinite height between $\mathcal{L}$ and $\mathcal{B}$ as well as between $\mathcal{R}$ and $\mathcal{B}$, i.e. in $\mathsf{L}_{\mathcal{LB}}$ and $\mathsf{L}_{\mathcal{BR}}$ (figure 1, top). In a tight-binding scheme, this corresponds to setting the respective hopping-matrix elements to zero.

2.1.2. The coupled system. The coupled system is described by the Hamiltonian $H_{\mathrm{c}} = H_{\mathrm{dc}} + \Delta V$, with the coupling between the subsystems established by the potential change ΔV (dashed regions in figure 2, bottom),

$$\Delta V = \begin{pmatrix} 0 & v_{\mathcal{LB}} & 0 \\ v_{\mathcal{BL}} & 0 & v_{\mathcal{BR}} \\ 0 & v_{\mathcal{RB}} & 0 \end{pmatrix}, \tag{3}$$

with $v_{\mathcal{LB}} = v_{\mathcal{BL}}^{\dagger}$ and $v_{\mathcal{RB}} = v_{\mathcal{BR}}^{\dagger}$. There is no direct connection between $\mathcal{L}$ and $\mathcal{R}$. The resolvent $G_{\mathrm{c}} = (z - H_{\mathrm{c}})^{-1}$ reads

$$G_{\mathrm{c}}(z) = \begin{pmatrix} g_{\mathcal{LL}}(z) & g_{\mathcal{LB}}(z) & g_{\mathcal{LR}}(z) \\ g_{\mathcal{BL}}(z) & g_{\mathcal{BB}}(z) & g_{\mathcal{BR}}(z) \\ g_{\mathcal{RL}}(z) & g_{\mathcal{RB}}(z) & g_{\mathcal{RR}}(z) \end{pmatrix}. \tag{4}$$

Note that the resolvents of the coupled (decoupled) subsystems are indicated by two subscripts (a single subscript).

The coupling is established by replacing the infinitely high potentials walls of the decoupled system by lead potentials in $\mathsf{L}_{\mathcal{LB}}$ and $\mathsf{L}_{\mathcal{BR}}$ (figure 2, top). In a tight-binding scheme, the coupling can be achieved by setting the hopping matrix elements between $\mathcal{L}$ and $\mathcal{B}$ as well as between $\mathcal{R}$ and $\mathcal{B}$ nonzero.

2.1.3. Self-energies and transition operators. The self-energy $\sigma(z)$ which describes the coupling of the isolated subsystem $\mathcal{B}$ to the leads $\mathcal{L}$ and $\mathcal{R}$, via the Dyson equation

$$g_{\mathcal{BB}}(z) = g_{\mathcal{B}}(z) + g_{\mathcal{B}}(z)\sigma(z)g_{\mathcal{BB}}(z), \tag{5}$$

is obtained from $(z - H_{\mathrm{c}})\, G_{\mathrm{c}}(z) = 1$ and reads

$$\sigma(z) = \sigma_{\mathcal{L}}(z) + \sigma_{\mathcal{R}}(z), \tag{6}$$

with $\sigma_{\mathcal{S}}(z) = v_{\mathcal{BS}}\, g_{\mathcal{S}}(z)\, v_{\mathcal{SB}}$ for $\mathcal{S} = \mathcal{L}, \mathcal{R}$.

The transition operators $t_{\mathcal{LR}}(z)$ and $t_{\mathcal{RL}}(z)$ which describe the transmission through the barrier $\mathcal{B}$ are obtained from $T(z) = \Delta V + \Delta V\, G_{\mathrm{c}}(z)\, \Delta V$,

$$t_{\mathcal{LR}}(z) = v_{\mathcal{LB}}\, g_{\mathcal{BB}}(z)\, v_{\mathcal{BR}}, \tag{7a}$$

$$t_{\mathcal{RL}}(z) = v_{\mathcal{RB}}\, g_{\mathcal{BB}}(z)\, v_{\mathcal{BL}}. \tag{7b}$$

2.1.4. Connection to the Landauer–Büttiker theory. The transmission $\Theta(\epsilon)$ from $\mathcal{L}$ to $\mathcal{R}$ (or vice versa) is given by [32]

$$\Theta(\epsilon) = \mathrm{Tr}\left[\gamma^{+}_{\mathcal{L}}(\epsilon)\, g^{+}_{\mathcal{BB}}(\epsilon)\, \gamma^{+}_{\mathcal{R}}(\epsilon)\, g^{-}_{\mathcal{BB}}(\epsilon)\right], \tag{8}$$

where (for $\mathcal{S} = \mathcal{L}, \mathcal{R}$)

$$\gamma^{\pm}_{\mathcal{S}}(\epsilon) = \frac{\mathrm{i}}{2\pi}\left[\sigma^{\pm}_{\mathcal{S}}(\epsilon) - \left(\sigma^{\pm}_{\mathcal{S}}(\epsilon)\right)^{\dagger}\right] = \frac{\mathrm{i}}{2\pi} v_{\mathcal{BS}}\left[g^{\pm}_{\mathcal{S}}(\epsilon) - g^{\mp}_{\mathcal{S}}(\epsilon)\right] v_{\mathcal{SB}}. \tag{9}$$

Here, we have introduced the side limits $g^{\pm}_{\mathcal{S}}(\epsilon) = \lim_{\eta\to 0^{+}} g_{\mathcal{S}}(\epsilon \pm \mathrm{i}\eta)$, with ϵ and positive η real. Representing $g^{\pm}_{\mathcal{S}}(\epsilon)$ by

$$g^{\pm}_{\mathcal{S}}(\epsilon) = \lim_{\eta\to 0^{+}} \sum_{l} \frac{|\phi^{(l)}_{\mathcal{S}}\rangle\langle\phi^{(l)}_{\mathcal{S}}|}{\epsilon \pm \mathrm{i}\eta - \epsilon^{(l)}_{\mathcal{S}}}, \tag{10}$$

where $|\phi^{(l)}_{\mathcal{S}}\rangle$ is an eigenstate of $h_{\mathcal{S}}$ with energy $\epsilon^{(l)}_{\mathcal{S}}$, yields

$$g^{+}_{\mathcal{S}}(\epsilon) - g^{-}_{\mathcal{S}}(\epsilon) = -2\pi\mathrm{i} \sum_{l} |\phi^{(l)}_{\mathcal{S}}\rangle\langle\phi^{(l)}_{\mathcal{S}}|\, \delta(\epsilon - \epsilon^{(l)}_{\mathcal{S}}). \tag{11}$$

Inserting all expressions into equation (8), one obtains

$$\Theta(\epsilon) = \sum_{l,r} \left|\langle\phi^{(l)}_{\mathcal{L}}|t^{+}_{\mathcal{LR}}(\epsilon)|\phi^{(r)}_{\mathcal{R}}\rangle\right|^{2} \delta(\epsilon - \epsilon^{(l)}_{\mathcal{L}})\, \delta(\epsilon - \epsilon^{(r)}_{\mathcal{R}}), \tag{12}$$

which establishes the connection to the result of Landauer and Büttiker. The latter express the conductance C as the sum over the transmission probabilities $\theta^{(lr)}_{\mathcal{LR}}$ of all pairs of scattering channels $|\phi^{(l)}_{\mathcal{L}}\rangle$ incoming in $\mathcal{L}$ and $|\phi^{(r)}_{\mathcal{R}}\rangle$ outgoing in $\mathcal{R}$,

$$C = \frac{e^2}{h} \sum_{l,r} \theta^{(lr)}_{\mathcal{LR}}(\epsilon) = \frac{e^2}{h}\Theta(\epsilon). \tag{13}$$

Here, $\theta^{(lr)}_{\mathcal{LR}}$ is identified with

$$\left|\langle\phi^{(l)}_{\mathcal{L}}|t^{+}_{\mathcal{LR}}(\epsilon)|\phi^{(r)}_{\mathcal{R}}\rangle\right|^{2} \delta(\epsilon - \epsilon^{(l)}_{\mathcal{L}})\, \delta(\epsilon - \epsilon^{(r)}_{\mathcal{R}}) \tag{14}$$

from equation (12).

The separation of the entire systems in individual subsystems, namely $\mathcal{L}$, $\mathcal{B}$ and $\mathcal{R}$, is essential only for the general formulation of the problem. In an actual implementation, one would skip this decomposition and deal only with the decoupled and the coupled system as a whole (see the following sections 2.2 and 2.3). Hence, the subsystems as well as $\mathsf{L}_{\mathcal{LB}}$ and $\mathsf{L}_{\mathcal{BR}}$ show up as ranges of sites (in conventional KKR) or as ranges of layers (in layer KKR), as being sketched in figures 1 and 2.

2.2. Formulation in KKR

The above general outline provides a realization of the Landauer–Büttiker theory in terms of Green functions which relies on two systems, the decoupled one and the coupled one. In accordance with the preceding remark, a formulation in terms of the entire systems, not in terms of the subsystems, is used now. The respective quantities are indexed by 'dc' and 'c' for the decoupled and the coupled system, respectively.

The essential ingredient is the complete decoupling of the subsystems which can easily be achieved in a tight-binding approach by modification of the hopping matrix elements. In KKR, however, one has direct access mainly to the (muffin-tin) potentials of the sites. Therefore, the decoupling can be obtained by erecting potential walls between the leads and the barrier in $\mathsf{L}_{\mathcal{LB}}$ and $\mathsf{L}_{\mathcal{BR}}$. By this means, the 'impermeable membrane' [26] is replaced by a barrier of finite width and finite height. Note that the residual coupling of the electronic states on either side of the decoupling barrier induces an error in the conductance calculations which, however, can in principle be made as small as wanted [26]. Further, the systems (coupled and decoupled) are identical except for the potentials in $\mathsf{L}_{\mathcal{LB}}$ and $\mathsf{L}_{\mathcal{BR}}$.

In KKR, the decoupling can be realized by a few layers with constant muffin-tin potentials of finite height (i.e. a potential wall made of so-called 'empty spheres'), v^i_{PW} for site i. In the coupled system, this potential has then to be replaced by the potential v^i_{c}. In other words, the potential change ΔV which establishes the coupling reads (equation (3))

$$\Delta v^i = v^i_{\mathrm{c}} - v^i_{\mathrm{PW}}, \qquad i \in \mathsf{L}_{\mathcal{LB}}, \mathsf{L}_{\mathcal{BR}}. \tag{15}$$

A KKR Green function $G(z)$ can be written as

$$\langle \boldsymbol{r}_i | G(z) | \boldsymbol{r}'_j \rangle = \sum_{\Lambda\Lambda'} \langle \boldsymbol{r}_i | Z^{\mathrm{R}i}_{\Lambda}(z) \rangle \tau^{ij}_{\Lambda\Lambda'}(z) \langle Z^{\mathrm{L}j}_{\Lambda'}(z) | \boldsymbol{r}'_j \rangle, \tag{16}$$

with site indices $i \neq j$ and z being a complex number. The scattering between site i and j is accounted for by the scattering-path operator $\tau^{ij}_{\Lambda\Lambda'}(z)$ which is given in spin-angular-momentum representation, i.e. $\Lambda = (\kappa\mu)$ in the relativistic or $\Lambda = (lms)$ in the nonrelativistic case [5, 33]. The left-hand-side (superscript L) and right-hand-side (superscript R) regular scattering solutions of the sites with potential v^i and v^j are denoted $\langle Z^{\mathrm{L}j}_{\Lambda'}(z)|$ and $|Z^{\mathrm{R}i}_{\Lambda}(z)\rangle$, respectively [34]. Note that the single-site part of the Green function (which should appear for $i = j$) is not needed because (i) both $\gamma_{\mathcal{L}}$ and $\gamma_{\mathcal{R}}$ contain the imaginary part of the Green function (equation (9)). The single-site part can be chosen real (for real energies) and, therefore, does not contribute. And (ii), $g_{\mathcal{BB}}$ is evaluated at either side of the tunnel barrier, implying $i \neq j$ (equation (8)).

It is convenient to reformulate equation (16) in vector and matrix notation [5, 35],

$$G^{ij}(z) = \boldsymbol{Z}^{\mathrm{R}i}(z) \boldsymbol{\tau}^{ij}(z) \boldsymbol{Z}^{\mathrm{L}j}(z), \tag{17}$$

where

$$(\boldsymbol{Z}^{\mathrm{R}i}(z))_{\Lambda} = |Z^{\mathrm{R}i}_{\Lambda}(z)\rangle, \tag{18a}$$

$$(\boldsymbol{Z}^{\mathrm{L}j}(z))_{\Lambda'} = \langle Z^{\mathrm{L}j}_{\Lambda'}(z)| \tag{18b}$$

appear as row and column vectors, respectively, and

$$(\boldsymbol{\tau}^{ij}(z))_{\Lambda\Lambda'} = \tau^{ij}_{\Lambda\Lambda'}(z) \tag{19}$$

defines a matrix. By this means, the Green functions of the decoupled (subscript dc, scattering-path operator $\boldsymbol{\lambda}^{ij}$) and the coupled system (subscript c, scattering-path operator $\boldsymbol{\mu}^{ij}$) can be expressed as

$$G^{ij}_{\mathrm{dc}}(z) = \boldsymbol{Z}^{\mathrm{R}i}_{\mathrm{dc}}(z) \boldsymbol{\lambda}^{ij}(z) \boldsymbol{Z}^{\mathrm{L}j}_{\mathrm{dc}}(z), \tag{20a}$$

$$G^{ij}_{\mathrm{c}}(z) = \boldsymbol{Z}^{\mathrm{R}i}_{\mathrm{c}}(z) \boldsymbol{\mu}^{ij}(z) \boldsymbol{Z}^{\mathrm{L}j}_{\mathrm{c}}(z). \tag{20b}$$

Further, the asymptotics for large radial coordinate ($r \to \infty$) of the rhs scattering solutions [5, 34] read

$$\boldsymbol{Z}^{\mathrm{R}i}(kr) \to \boldsymbol{j}^{\mathrm{R}}(kr)\left[\boldsymbol{t}^{\mathrm{R}i}(kr)\right]^{-1} - \mathrm{i}k\boldsymbol{h}^{\mathrm{R}}(kr), \tag{21}$$

with vectors $\boldsymbol{j}^{\mathrm{R}}$ and $\boldsymbol{h}^{\mathrm{R}}$ defined in terms of spherical Bessel and Hankel functions [36], respectively, $\boldsymbol{t}^{\mathrm{R}i}$ being the rhs single-site scattering matrix of site i, and the wavenumber k at energy ϵ.

The operator trace in equation (8) translates in KKR into a sum over sites i, a sum over spin-angular-momenta Λ and a spatial integration over muffin-tin spheres. According to equations (9) and (15), the summation over sites can be restricted to $\mathsf{L}_{\mathcal{LB}}$ and $\mathsf{L}_{\mathcal{BR}}$. In these regions, the integration over muffin-tin spheres leads to terms like

$$(\boldsymbol{\Delta t}^{\mathrm{R}i})_{\Lambda\Lambda'} = \langle Z^{\mathrm{L}i}_{\mathrm{c}\Lambda}|\Delta v^i|Z^{\mathrm{R}i}_{\mathrm{dc}\Lambda'}\rangle. \tag{22}$$

which can be expressed by means of the single-site scattering matrices $\boldsymbol{t}^{\mathrm{R}i}_{\mathrm{c}}$ and $\boldsymbol{t}^{\mathrm{R}i}_{\mathrm{PW}}$ of v^i_{c} and v^i_{PW}, respectively,

$$\boldsymbol{\Delta t}^i = \boldsymbol{t}^{\mathrm{R}i}_{\mathrm{c}} - \boldsymbol{t}^{\mathrm{R}i}_{\mathrm{PW}}. \tag{23}$$

Taking all scattering-path operators at ϵ^+, equation (8) is eventually expressed as

$$\Theta(\epsilon) = -\sum_{lm}^{\mathsf{L}_{\mathcal{LB}}}\sum_{no}^{\mathsf{L}_{\mathcal{BR}}} \boldsymbol{\Delta t}^l\left[\boldsymbol{\lambda}^{lm} - (\boldsymbol{\lambda}^{ml})^\dagger\right](\boldsymbol{\Delta t}^m)^\dagger\boldsymbol{\mu}^{mn}\boldsymbol{\Delta t}^n\left[\boldsymbol{\lambda}^{no} - (\boldsymbol{\lambda}^{on})^\dagger\right](\boldsymbol{\Delta t}^o)^\dagger(\boldsymbol{\mu}^{lo})^\dagger. \tag{24}$$

In systems with translational symmetry parallel to the tunnel barrier (e.g. planar tunnel junctions), the in-plane wavevector $\boldsymbol{k}_\parallel$ is conserved in the tunnel process. Thus, the above expressions for the Green functions and the transmission (equations (3) and (24)) hold for each $\boldsymbol{k}_\parallel$. To obtain the conductance C one has to integrate over the two-dimensional Brillouin zone (2BZ),

$$C = \frac{e^2}{h}\int_{2\mathrm{BZ}} \Theta(\epsilon, \boldsymbol{k}_\parallel)\,\mathrm{d}k^2. \tag{25}$$

2.3. Implementation notes

In our relativistic layer-KKR computer code, three methods for computing the conductance of a planar tunnel junction were implemented: the MacLaren–Butler approach of Bloch-wave transmission (abbreviated BW, for Bloch-wave transmission) [19], the tight-binding-like approach presented here (TB) and the Kubo–Greenwood-based approach proposed by Mavropoulos *et al* (KG) [17]. In our scalar-relativistic screened-KKR computer code the TB approach was implemented as well [37].

A self-consistent calculation has to be performed only for the coupled system. The decoupled system can be treated non-self-consistently because it can be regarded as an auxiliary system, needed only for the 'counting of transmitted electrons' idea inherent in the Landauer–Büttiker theory. The actual electronic structure in the vicinity of the decoupling potentials, described by the 'surface Green functions' of the leads, is accounted for by the self-energies. Thus, the actual shape of the decoupling potentials should not matter, at least in principle (i.e. provided that the decoupling is complete).

In the decoupled system, the electronic states of both the lead and the tunnel-barrier side decay exponentially in $\mathsf{L}_{\mathcal{LB}}$ and $\mathsf{L}_{\mathcal{BR}}$. In the spirit of the Landauer–Büttiker theory, one has to couple to the Bloch states in the leads, not to the states originating from the tunnel barrier $\mathcal{B}$. Thus, it appears preferable to sum only over those sites in $\mathsf{L}_{\mathcal{LB}}$ and $\mathsf{L}_{\mathcal{BR}}$ (equation (24)) that are close to the leads $\mathcal{L}$ and $\mathcal{R}$, respectively, rather than close to the tunnel barrier. This restriction was found to slightly improve the conductance results.

The decoupling can be checked by considering the conductance of an ideal lead (without tunnel barrier; see section 3.1), for which the transmission is equal to the number of scattering channels. The demanded decoupling potential can be obtained by increasing the number of separating layers (i.e. the ranges of $\mathsf{L}_{\mathcal{LB}}$ and $\mathsf{L}_{\mathcal{BR}}$) and by adjusting the height of the potential wall v_{PW}. It is found that typically seven layers with potentials of 54.42 eV (2.00 H) height are sufficient.

By putting $\mathsf{L}_{\mathcal{LB}}$ and $\mathsf{L}_{\mathcal{BR}}$ far into the leads, conduction via interface states, which are located at the boundaries of the tunnel barrier and have energies within a bandgap of the respective lead, can be ruled out. However, by locating these regions close to the actual tunnel barrier, the effect of localized states on the conductance can be taken into account [28, 38].

3. Results and discussion

3.1. Comparison with other approaches

For the tests with the layer-KKR code in relativistic mode, an fcc lattice with Cu lattice constant was chosen, with the layers normal to the [001] direction. The spin-dependent muffin-tin potentials of the leads $\mathcal{L}$ and $\mathcal{R}$ were chosen to be constant with depths of -4.08 eV (-0.15 H) for spin-up and -2.72 eV (-0.10 H) for spin-down electrons, respectively. The decoupling potential walls were chosen to be five layers wide and of height 54.42 eV (2.00 H). This set-up leads to a nearly-free-electron band structure with small band gaps at $\boldsymbol{k}_{\parallel} = 0$ (arrows in figure 3(a)). The imaginary part η of the energy was chosen to be 10^{-6} eV.

3.1.1. Conductance of the bare leads. Having identical leads with no tunnel barrier in between, the transmission $\Theta(\epsilon, \boldsymbol{k}_{\parallel})$ equals the number of scattering channels at energy ϵ and in-plane wavevector $\boldsymbol{k}_{\parallel}$. Since the BW approach reproduces perfectly these integer numbers (black in figure 3(b)), its results were taken as a reference for all tests. The maximum angular momentum in the KKR expansion was $l_{\max} = 2$.

As is evident from figure 3(b), the TB method nicely reproduces the number of Bloch states, i.e. the BW result. In the scale of the figure, the data for the BW and TB approach coincide. Note the reduction of the transmission at the band gaps at about 7.5 eV (spin-up) and 8.9 eV (spin-down). With increasing energy, the wavefunctions decay less in the potential walls and the decoupling should become worse. However, the deviation of Θ_{TB} from Θ_{BW} does not increase considerably. In contrast, the KG approach reveals significant deviations in the entire energy range (except for energies below -1 eV), observed by other groups, too [39]. In order to come closer to the reference data, the maximum angular momentum $l_{\max}$ was increased, which improves the current-matrix elements. An increase from $l_{\max} = 2$ (used for the BW and the TB calculations) to $l_{\max} = 4$ improves the results for energies below 18.8 eV but still leaves a considerable discrepancy at higher energies, in particular at the onset of the bands at about 19 eV. (In order to overcome this problem, one could increase $l_{\max}$ even further, thereby increasing the computation time, too. The spatial integration of the current-matrix elements was performed over five monolayers in each of the leads, resulting in converged transmissions with respect to this parameter [17].)

In order to provide a measure for the deviation from the BW results, the relative error

$$\Delta\Theta_{\mathrm{X}}(\epsilon, \boldsymbol{k}_{\parallel}) = \frac{\Theta_{\mathrm{X}}(\epsilon, \boldsymbol{k}_{\parallel}) - \Theta_{\mathrm{BW}}(\epsilon, \boldsymbol{k}_{\parallel})}{\Theta_{\mathrm{BW}}(\epsilon, \boldsymbol{k}_{\parallel})}, \qquad \mathrm{X} = \mathrm{TB}, \mathrm{KG}, \tag{26}$$

will be addressed (figure 3(c)). Although an increase of $l_{\max}$ improves the result, the error of the KG approach renders this method not satisfying, at least in our implementation. In contrast, the

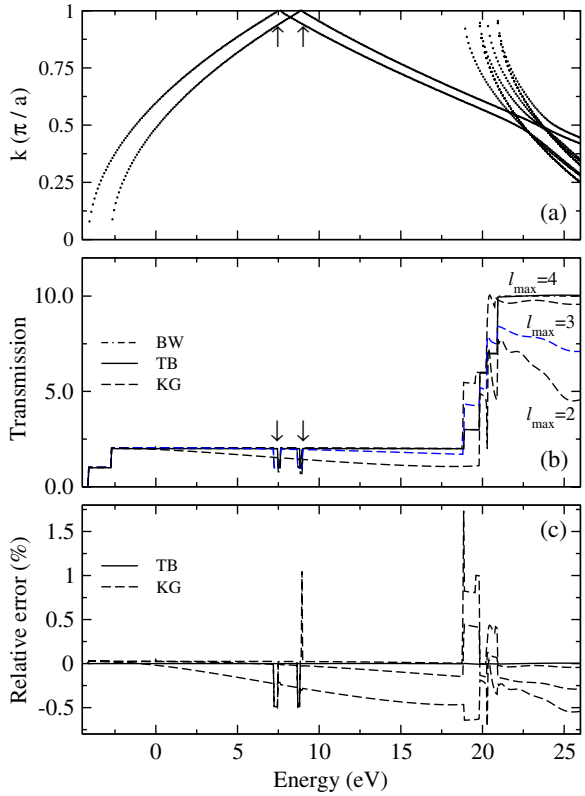

Figure 3. Conductance of the bare-lead model system. (a) Exchange-split bandstructure $E(k)$ of the leads for $\boldsymbol{k}_\parallel = 0$ (a denoting the lattice constant). Arrows mark bandgaps discussed in the text. (b) Transmission Θ versus energy at $\boldsymbol{k}_\parallel = 0$ for the BW (dashed–dotted), the TB (solid) and the KG approach (dashed). For the latter, three datasets with maximum angular momentum $l_{\max} = 2$, 3 and 4 are shown (as indicated on the right). The bandgaps of (a) are marked in addition. (c) Relative errors $\Delta\Theta$ with respect to the BW approach (equation (26)).

(This figure is in colour only in the electronic version)

maximum relative error of the TB method in the entire range of energies is less than $7 \times 10^{-3}\%$, indicating this approach as reliable.

3.1.2. Conductance of a rectangular barrier. For a second test, the muffin-tin potentials of two layers in $\mathcal{B}$ were replaced by constant walls of 6.80 eV height (0.25 H), this way introducing the KKR equivalent of a rectangular tunnel barrier. Here, $l_{\max} = 4$ was used for all approaches.

Both Green function approaches (TB and KG) reproduce the general shape of the transmission well (figure 4(a)). The transmission increases from almost zero to about 2 at energies around 8 eV. The two sharp minima are due to the aforementioned band gaps (see figure 3(a)). While the TB results are indistinguishable from the reference data, the KG data show eye-catching deviations at about 10 eV. These findings are reflected in the relative error: the mean deviations are about 0.02% and $2 \times 10^{-5}\%$ for the KG and the TB approach, respectively.

In the computations report above, the decoupling potential walls were located directly at the tunnel barrier, i.e. there were no layers with lead potentials separating the decoupling barrier

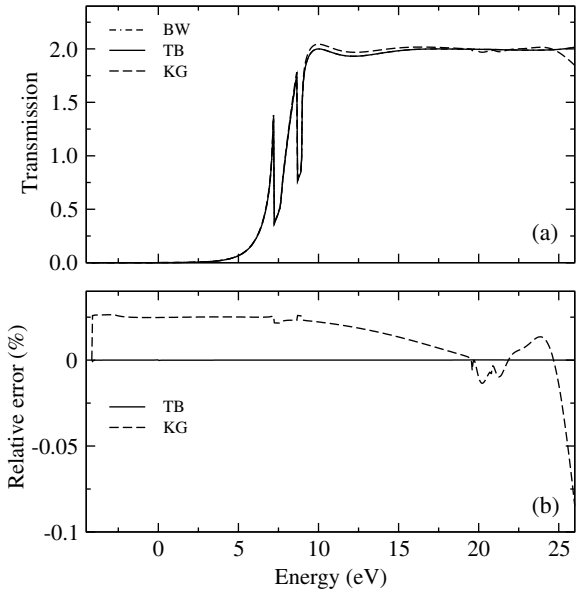

Figure 4. Conductance of the rectangular-barrier model system. (a) Transmissions Θ versus energy at $\boldsymbol{k}_{\parallel} = 0$ for the discussed approaches (line styles as in figure 3). (b) Relative errors $\Delta\Theta$ with respect to the BW approach.

from the tunnel barrier. Separating the two barriers from each other by three layers with lead potentials did not significantly change the transmission.

3.1.3. Conclusions. The results for the simple model systems and for further tests not presented here give strong evidence that the TB method is as accurate and reliable as the BW method. In contrast, the accuracy of the KG approach is significantly worse, at least as it is implemented in our layer-KKR code. Similar problems with the KG method implemented in other KKR computer codes are reported, the problems being traced back to the computation of the current-matrix elements [39]. In calculations for realistic systems, like Fe/MgO/Fe tunnel junctions, the conductance becomes very small, in particular several orders of magnitude less than in the tests reported here [11, 13]. Within this respect, a reliable and highly accurate computational scheme is absolutely essential.

3.2. Screened KKR: Influence of the screening transformation

One of the main difficulties of the conventional KKR method is the long-range behaviour of the structure constants, which leads to numerical complications for large systems. This problem can be overcome by using so-called screened structure constants which, according to the concept of screening [40], decay exponentially in configuration space. The screened structure constants can be easily Fourier-transformed to any dimensionality and are used in order-N methods for electronic-structure calculations of extended systems. The screened version of KKR has become a standard for electronic-structure calculations for large three- and two-dimensional systems (see for example [37, 41–50]).

The screening transformation in KKR is defined by the Dyson equation [42, 43]

$$\boldsymbol{G}^{\alpha}(z) = \boldsymbol{G}^{0}(z)\left[\mathbf{1} - \boldsymbol{\alpha}(z)\boldsymbol{G}^{0}(z)\right]^{-1}, \tag{27}$$

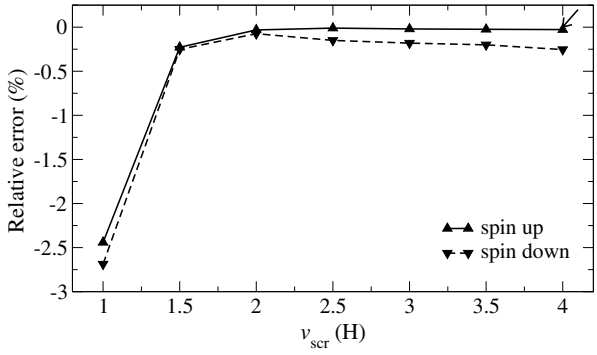

Figure 5. Spin-resolved transmissions of a bare Fe(001) lead. The relative error $\Delta\Theta_{TB}$ versus height of the screening potential v_{scr} is shown for spin-up (solid, upright triangles) and spin-down (dashed, downward triangles) electrons [$\boldsymbol{k}_\parallel = 0$, $E = E_F$, $l_{max} = 2$ and $r_{cl} = 2.2\,a_{latt}$ ($n_{cl} = 89$)]. Data for $v_{scr} = 4$ H obtained with $l_{max} = 4$ are indicated by the arrow in the top-right corner.

where $\boldsymbol{G}^0(z)$ are conventional KKR structure constants. The screening parameters are comprised in a supermatrix $\boldsymbol{\alpha}(z)$ which is diagonal in the spin-angular-momentum components Λ and in the site indices i,

$$(\boldsymbol{\alpha}(z))^{ij}_{\Lambda\Lambda'} = \alpha^i_l(z)\delta_{\Lambda\Lambda'}\delta_{ij}. \tag{28}$$

The Green function of the realistic system is eventually calculated from the Dyson equation with respect to the new reference system, i.e. that with the screened structure constants $\boldsymbol{G}^\alpha$.

The standard choice of the screening parameters $\alpha(z)$, being established over the years, is single-site path operators of a system with potential walls (i.e. repulsive 'empty spheres' with potential v^α) placed at each site. The scattering-path operator of the reference systems decays exponentially in configuration space, allowing for an efficient numerical treatment due to the tridiagonal form of the involved matrices.

In principle, the screening transformation is exact, but in practice one defines a cluster around each site and calculates the scattering-path operator of the reference system in configurational space. Because the scattering-path operator is set to zero outside the cluster, the screening transformation is no longer exact. Its accuracy depends on three parameters: the size of the cluster, the repulsive potential v^α and the maximum angular momentum l_{max}, all of which define the decay strength of the screened structure constants.

To test the influence of the screening on the conductance, bare Fe(001) leads, without a tunnel barrier in between, were chosen. The decoupling potential v_{PW} was taken to be 54.42 eV (2.00 H) high and six layers wide in both $\mathsf{L}_{\mathcal{LB}}$ and $\mathsf{L}_{\mathcal{BR}}$. For $\boldsymbol{k}_\parallel = 0$, the number of scattering channels at the Fermi level E_F is 4 for each spin orientation (up and down). Using the layer-KKR code running in scalar-relativistic mode (which does not rely on screening), these numbers are very well reproduced by the BW and the TB approaches. In particular for the latter, one finds with $l_{max} = 3$ relative errors $\Delta\Theta_{TB}$ of -0.0087% and $+0.0033\%$ for spin-up and spin-down electrons, respectively.

3.2.1. Height of the screening potential. For $l_{max} = 2$ and a cluster size n_{cl} of 89 sites (seven atomic shells in the body-centred cubic lattice), the relative error $\Delta\Theta_{TB}$ of the transmission (equation (26)) was computed for v_{scr} between 1 H and 4 H (figure 5). For v_{scr} of 1 H height, the decay of the scattering-path operator of the reference system is too little, thus leading to inaccurate Green functions of the Fe leads. In total, this results in large $\Delta\Theta_{TB}$ (in absolute

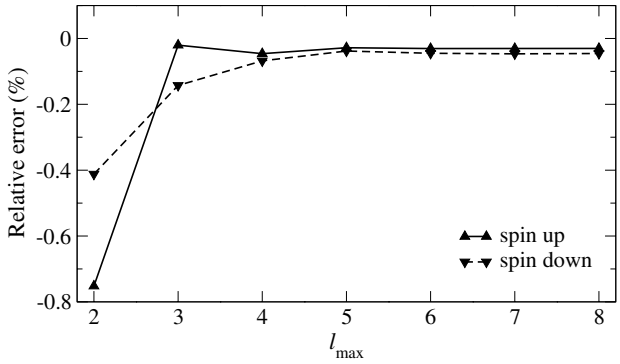

Figure 6. Spin-resolved transmissions of a bare Fe(001) lead. As figure 5, but for the relative error $\Delta\Theta_{TB}$ versus maximum angular momentum l_{max}. Line styles and symbols as in figure 5 ($\boldsymbol{k}_{\parallel} = 0$, $E = E_F$, $r_{cl} = 2.2\,a_{latt}$, $n_{cl} = 89$ and $v_{scr} = 2$ H).

value). An increase of v_{scr} reduces the error but too large a v_{scr} worsens the result, especially for the spin-down transmission. Summarizing, for a given l_{max} and r_{cl} there exists an optimal height of the screening potential.

A well-known feature of screened KKR is that an increase of v_{scr} should be accompanied by an increase of l_{max} in order maintain the screening. Hence, for $l_{max} = 4$ and $v_{scr} = 4$ H $\Delta\Theta_{TB}$ is reduced considerably in absolute value (from -0.027% (spin-up) and -0.25% (spin-down) for $l_{max} = 2$ to -0.010% (spin-up) and -0.010% (spin-down) for $l_{max} = 4$; see the arrow in figure 5).

3.2.2. Maximum angular momentum. As a second test, v_{scr} and n_{cl} were fixed to 2 H and 89 sites, respectively, while l_{max} was varied between 2 and 8 (figure 6). While $\Delta\Theta_{TB}$ of the spin-down transmission decreases monotonously (in absolute value) with increasing l_{max}, the spin-up transmission displays a modulation on top of the global decrease. Both errors appear converged for $l_{max} \geqslant 5$. Again, to minimize the error, one needs to find the optimal l_{max} (here, apparently $l_{max} = 5$).

3.2.3. Size of the screening cluster. The size of the cluster in which the scattering-path operator of the 'screened' reference system is nonzero can either be specified by the radius r_{cl} (given in units of the Fe lattice constant a_{latt}) of the spherical cluster around each site or by the number of sites n_{cl} within this sphere.

For this test, $v_{scr} = 2$ H and $l_{max} = 2$ were chosen while the size of the screening cluster r_{cl} was varied between $1.6\,a_{latt}$ and $2.6\,a_{latt}$ (figure 7). The cluster has to have a specific minimum size in order to establish the screening. In the present case, one needs $r_{cl} \geqslant 1.9$ ($n_{cl} \geqslant 59$). Reliable transmissions are obtained for $2.2 \leqslant r_{cl} \leqslant 2.5$, i.e. $89 \leqslant n_{cl} \leqslant 137$. A further increase of the cluster size does no reduce the error.

3.2.4. Conclusions. From the above considerations an optimal set of screening parameters was deduced. For $v_{scr} = 3$ H, $l_{max} = 3$ and $r_{cl} = 2.2\,a_{latt}$ (i.e. $n_{cl} = 89$), the relative errors were as small as -0.020% and -0.025% for the spin-up and the spin-down transmission, respectively.

The accuracy of the screening transformation can be essentially improved when the real-space structure constants are replaced by the $\boldsymbol{k}_{\parallel}$-projected $\boldsymbol{G}^0(z)$ (equation (27)), making the

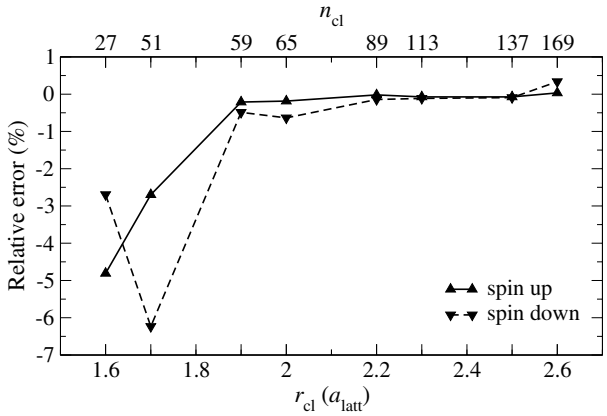

Figure 7. Spin-resolved transmissions of a bare Fe(001) lead. As figures 5 and 6, but for the relative error $\Delta\Theta_{TB}$ versus cluster size, the latter given by the cluster radius r_{cl} (bottom axis, in units of the Fe lattice constant a_{latt}) or by the number of sites n_{cl} within the cluster (top axis). Line styles and symbols as in figure 5 ($k_{\parallel} = 0$, $E = E_F$, $l_{max} = 2$ and $v_{scr} = 2$ H).

screening transformation exact in planes parallel to the layers and resulting in a lower sensitivity on the screening parameters [50]. In general, the accuracy improved by a factor of 10 and, therefore, the TB approach in screened KKR is as good as in layer KKR.

The tests prove that the TB approach is also suitable for screened-KKR methods: conductances computed within screened KKR can be made as accurate as without screening. However, one has to take care of the appropriate choice of the screening parameters for optimal results.

4. Concluding remarks

The results presented in this paper suggest an implementation of the tight-binding-inspired approach in KKR computer codes for electronic-structure calculations. It might also be implemented in codes which rely on localized basis sets (for example, linear-muffin-tin orbital (LMTO) codes). Further, it appears to be particularly useful as an alternative to existing computational schemes, giving the possibility to check numerical results which otherwise are hard to test.

Acknowledgments

Fruitful discussions with M Czerner, P M Levy, I Mertig and P Zahn are very much appreciated.

References

[1] Maekawa S and Shinjo T (ed) 2002 *Spin Dependent Transport in Magnetic Nanostructures* (London: Taylor and Francis)
[2] Imry Y and Landauer R 1999 *Rev. Mod. Phys.* **71** S306
[3] Korringa J 1994 *Phys. Rep.* **238** 341
[4] Mertig I, Mrosan E and Ziesche P 1987 *Multiple Scattering Theory of Point Defects in Metals: Electronic Properties* (Leipzig: Teubner)
[5] Weinberger P 1990 *Electron Scattering Theory of Ordered and Disordered Matter* (Oxford: Clarendon)

[6] Gonis A 1992 *Green Functions for Ordered and Disordered Systems* (*Studies in Mathematical Physics* vol 4) (Amsterdam: North-Holland)
[7] Popescu V, Ebert H, Papanikolaou N, Zeller R and Dederichs P H 2004 *J. Phys.: Condens. Matter* **16** S5579
[8] Wunnicke O, Mavropoulos P, Zeller R and Dederichs P H 2004 *J. Phys.: Condens. Matter* **16** 4643
[9] Dederichs P H, Mavropoulos P, Wunnicke O, Papanikolaou N, Bellini V, Zeller R, Drchal V and Kudrnovský J 2002 *J. Magn. Magn. Mater.* **240** 108
[10] Mavropoulos P, Wunnicke O and Dederichs P H 2002 *Phys. Rev.* B **66** 024416
[11] Butler W H, Zhang X G, Schulthess T C and MacLaren J M 2001 *Phys. Rev.* B **63** 054416
[12] Zhang X G and Butler W H 2003 *J. Phys.: Condens. Matter* **15** R1603
[13] Zhang X G, Butler W H and Bandyopadhyay A 2003 *Phys. Rev.* B **68** 092402
[14] Henk J and Bruno P 2003 *Phys. Rev.* B **68** 174430
[15] Palotás K, Lazarovits B, Szunyogh L and Weinberger P 2003 *Phys. Rev.* B **67** 174404
[16] Weinberger P, Levy P, Banhart J, Szunyogh L and Újfalussy B 1996 *J. Phys.: Condens. Matter* **8** 7677
[17] Mavropoulos P, Papanikolaou N and Dederichs P H 2004 *Phys. Rev.* B **69** 125104
[18] Büttiker M 1986 *Phys. Rev. Lett.* **57** 1761
[19] MacLaren J M, Zhang X G, Butler W H and Wang X 1999 *Phys. Rev.* B **59** 5470
[20] Henk J 2001 *Handbook of Thin Film Materials* vol 2, ed H S Nalwa (San Diego, CA: Academic) chapter 10, p 479
[21] Soven P 1967 *Phys. Rev.* **156** 809
[22] Velický B 1969 *Phys. Rev.* **184** 614
[23] Butler W H 1985 *Phys. Rev.* B **31** 3260
[24] Velev J and Butler W H 2005 *J. Appl. Phys.* **97** 10C517
[25] Mathon J and Umerski A 2001 *Phys. Rev.* B **63** 220403
[26] Pendry J B, Prête A B and Krutzen B C H 1991 *J. Phys.: Condens. Matter* **3** 4313
[27] Zhang S and Levy P M 1989 *Eur. Phys. J.* B **10** 599
[28] Wang K, Levy P M, Zhang S and Szunyogh L 2003 *Phil. Mag.* **83** 1255
[29] Inglesfield J E 1971 *J. Phys. C: Solid State Phys.* **4** L14
[30] Wortmann D, Bihlmayer G and Blügel S 2004 *J. Phys.: Condens. Matter* **16** S5819
[31] Davies O R and Inglesfield J E 2004 *Phys. Rev.* B **69** 195110
[32] Fisher D S and Lee P A 1981 *Phys. Rev.* B **23** 6851
[33] Rose E M 1961 *Relativistic Electron Theory* (New York: Wiley)
[34] Tamura E 1992 *Phys. Rev.* B **45** 3271
[35] Zabloudil J, Hammerling R, Szunyogh L and Weinberger P (ed) 2005 *Electron Scattering in Solid Matter* (Berlin: Springer)
[36] Abramowitz M and Stegun I A (ed) 1970 *Handbook of Mathematical Functions* (New York: Dover)
[37] Lüders M, Ernst A, Temmerman W M, Szotek Z and Durham P J 2001 *J. Phys.: Condens. Matter* **13** 8587
[38] Levy P M, Wang K, Dederichs P H, Heide C, Zhang S and Szunyogh L 2002 *Phil. Mag.* B **82** 763
[39] Zahn P 2005 private communication
[40] Andersen O K and Jepsen O 1984 *Phys. Rev. Lett.* **53** 2571
[41] Szunyogh L, Újfalussy B, Weinberger P and Kollár J 1994 *J. Phys.: Condens. Matter* **6** 3301
[42] Szunyogh L, Újfalussy B, Weinberger P and Kollár J 1994 *Phys. Rev.* B **49** 2721
[43] Zeller R, Dederichs P H, Újfalussy B, Szunyogh L and Weinberger P 1995 *Phys. Rev.* B **52** 8807
[44] Zeller R 1997 *Phys. Rev.* B **55** 9400
[45] Schwitalla J and Györffy B L 1998 *J. Phys.: Condens. Matter* **10** 10995
[46] Zahn P, Mertig I, Zeller R and Dederichs P H 1998 *Phil. Mag.* B **78** 411
[47] Moghadam N Y, Stocks G M, Újfalussy B, Shelton W A, Gonis A and Faulkner J S 1999 *J. Phys.: Condens. Matter* **11** 5505
[48] Petit L, Beiden S V, Temmerman W M, Szotek Z, Stocks G M and A G G 2000 *J. Phys.: Condens. Matter* **12** 8439
[49] Wildberger K, Zeller R and Dederichs P H 1997 *Phys. Rev.* B **55** 10 074
[50] Uiberacker C, Szunyogh L, Újfalussy B, Weinberger P, Ernst A and Dederichs P H 1998 *Phil. Mag.* B **78** 423